World Academy of Science, Engineering and Technology
International Journal of Materials and Metallurgical Engineering
Vol:10, No:5, 2016

Submicron Size of Alumina/Titania Tubes for CO_2-CH_4 Conversion

Chien-Wan Hun, Shao-Fu Chang, Jheng-En Yang, Chien-Chon Chen, Wern-Dare Jheng

***Abstract*—**This research provides a systematic way to study and better understand double nano-tubular structure of alunina (Al_2O_3) and titania (TiO_2). The TiO_2 NT was prepared by immersing Al_2O_3 template in 0.02 M titanium fluoride (TiF_4) solution (pH=3) at 25 °C for 120 min, followed by annealing at 450 °C for 1 h to obtain anatase TiO_2 NT in the Al_2O_3 template. Large-scale development of film for nanotube-based CO_2 capture and conversion can potentially result in more efficient energy harvesting. In addition, the production process will be relatively environmentally friendly. The knowledge generated by this research will significantly advance research in the area of Al_2O_3, TiO_2, CaO, and Ca_2O_3 nano-structure film fabrication and applications for CO_2 capture and conversion. This green energy source will potentially reduce reliance on carbon-based energy resources and increase interest in science and engineering careers.

***Keywords*—**Alumina, titania, nano-tubular, film, CO_2.

I. Introduction

INCREASED energy demands and concerns about global warming compel scientists to keep looking for potential renewable energy sources unremittingly. At the Copenhagen United Nations Climate Change Conference, these issues were not passed over, but rather extended to another more positive topic—control of greenhouse gases, especially carbon dioxide. More and more frequent human activities not only reduce supplies of fossil fuel but have also rapidly increased anthropogenic carbon dioxide to a level of great concern. Seeking alternative energy sources may allow us to retain our quality of life. Furthermore, solving the CO_2 issue will alleviate future problems.

In 1979, Honda and co-workers demonstrated use of photovoltaic reactions to recycle carbon dioxide via conversion into organic compounds in water [1]; much additional research on photocatalytic conversion of carbon dioxide in liquids followed [2]-[4]. This reaction involves only water and carbon dioxide to form a useful carbon cycle:

$$CO_2 + 2H_2O \rightarrow CH_4 + 2O_2 \quad (1)$$

C.W. Hun is with the Department of Department of Mechanical Engineering, National United University, Miaoli, Taiwan (phone: +886-37-382309; fax:+886-37-382-326; e-mail: monger@nuu.edu.tw).

Shao-Fu Chang, Jheng-En Yang, and Chien-Chon Chen* are with the Department of Energy Engineering, National United University, Miaoli, Taiwan (phone: +886-37-382383; fax:+886-37-382-391; e-mail: shaofu78@gmail.com, a0953087075@gmail.com, ccchen@nuu.edu.tw).

Wern-Dare Jheng* is with the Department of Mechanical Engineering, National Chin-Yi University of Technology, Taichung, Taiwan (phone: +886-4-23924505 ext 7194; fax: +886-4-23930681; e-mail: jen102@ncut.edu.tw).

The photocatalytic hydrocarbon-forming reaction requires photons; hence, a significant hydrocarbon reaction yield requires a photocatalyst that utilizes solar energy efficiently. Graetzel et al. [5] reported the production of methane from a mixture of carbon dioxide and hydrogen by using a nano-particle dye sensitized solar cell (NP-DSSC) system.

Because there are two double bonds between C and O (C=O), where each C=O has 745 (kJ/mol) bonding energy [6], CO_2 conversion always requires extremely high pressure and/or high temperature. However, CO_2 that is converted via a TiO2 photocatalytic reduction process is relatively more manageable, allowing specific formation of compounds such as CH_4, CO, CH_3OH, HCHO, and HCOOH [7]. Ishitani [8] reported that platinum (Pt) dispersed on TiO_2 can improve the photocatalytic activity of TiO_2. Slamet [9] pointed out that copper ion (Cu^{2+}) supported on TiO_2 contributes significantly to improving CO2 photocatalytic reduction activity. According to Varghese's [10] research, CO concentration is higher on Cu surface-loaded samples and H_2 concentration is higher on Pt loaded samples, indicating that Cu is more active in reducing carbon dioxide ($2CO_2 + 4e^- \rightarrow 2CO + O_2$) while Pt prefers water reduction ($H_2O + h^+ \rightarrow {}^{\bullet}OH + H^+$). Also in Varghese's research, 6.8% conversion of carbon dioxide and water vapor to methane is achieved using nitrogen-doped titania nanotube arrays.

II. Experimental procedure

Aluminum foil (99.7%) was put inside the electrochemical holder forming AAO through electrolyte polishing and anodization in electrochemical bath. As described in Chen [11-13], AAO film can be fabricated using an anodization process. The fabrication processes for 15 nm AAO template consists of the following steps:

(i) Polish the aluminum (Al) substrate (99.7%); then anneal in an air furnace at 550℃.
(ii) Electro-polish the substrate in a bath consisting of $HClO_4$, C_2H_6O, and $CH_3(CH_2)_3OCH_2CH_2OH$ with 42 V DC for 10 minutes.
(iii) First anodization – Polish the Al substrate with 18 V DC in H_2SO_4 solution for 20 minutes.
(iv) Remove the first anodization film by soaking in a solution of CrO_3 and H_3PO_4 for 40 minutes.
(v) Second anodization – Repeat anodization using the solution from the first anodization, but for a longer time (several hours) to form AAO films of varying thickness.
(vi) Remove Al substrate by soaking in a solution of $CuCl_2$ and HCl for 30 minutes.

(vii) Widen pore diameter of AAO template using 5 vol.% H_3PO_4 solution for 20 minutes.

According to above steps when the voltage and electrolyte (step iii) are change to 40V and 3 wt.% $C_2H_2O_4$, and pore widening time is 70 min (step vii), that 60 nm pore size of AAO can be formed. As well as, when the voltage and electrolyte (step iii) are change to 195V and 1 vol.% H_3PO_4, and pore widening time is 200 min (step vii), that 300 nm pore size of AAO can be formed.

III. Results and Discussion

The fabrication of nanomaterials with controlled size and composition is of fundamental and technological interest. The template synthesis method can produce nanomaterials of uniform size easily. In using templates to produce nanostructures, one must take into account the template's chemical, mechanical, and thermal stability, its insulating properties, the minimal diameter and uniformity of the pores, and the pore density. Aluminum anodization is one of the most controllable self-assembly processes. Anodic aluminum oxide (AAO) has received much attention, because of its high aspect ratio, uniform pore size, and ordering nanopore dispersion. Additionally, it is stable in the chemical and thermal surrounding, and an inexpensive process for fabrication. Detail on the structure and preparation of alumina templates can be found elsewhere.

When anodized in an acidic electrolyte and controlled in the suitable conditions, aluminum forms a porous oxide with very uniform and parallel cell pores. Each cell contains an elongated cylindrical sub-micron or nanopore normal to the aluminum surface, extending from the surface of the oxide to the oxide/metal interface, where it is sealed by a thin barrier oxide layer with approximately hemispherical geometry.

Honeycomb structures with high aspect ratios on the nanometer scale have received interest for various applications. To obtain a nanochannel array as a template, nanoporous alumina formed by anodization has widely been studied for several decades. Aluminum in the presence of air or aqueous electrolytes is always covered with a thin natural layer of alumina. When a positive voltage is applied to an aluminum substrate in a suitable electrolyte, pores form on the surface at almost random positions. However, under specific conditions, almost perfect hexagonally ordered pores in anodic alumina can be obtained.

The anodizing oxide film of AAO consists of two layers: the porous thick outer layer (porous type) that grows on an inner layer (barrier type), which is thin, dense and dielectrically compact, and called the barrier layer, the active layer or the dielectric layer. The barrier layer is very thin, typically with a thickness of between 0.1 and 2% of that of the entire film. Depending on the various electrolytes, anodizing time, and anodizing voltage, AAO could be formed to compact alumina, thick porous alumina, or etching types. Compact alumina (no pores) was formed in a very weak acid or neutral solution, and thickness was determined by applied voltage. Thick porous alumina formed in a medium acid solution, and thickness was determined by anodizing time. Pore density increased when anodizing time increased, but decreased when anodizing voltage increased. For example, Fig. 1 showed the bottom images of AAO. (a) A dense barrier layer presents on the AAO bottom, (b) barrier layer was dissolved by H_3PO_4 solution and honeycomb structure of bottom AAO was presented. (c) AAO pores were enlarged after pore widening process by H_3PO_4 solution.

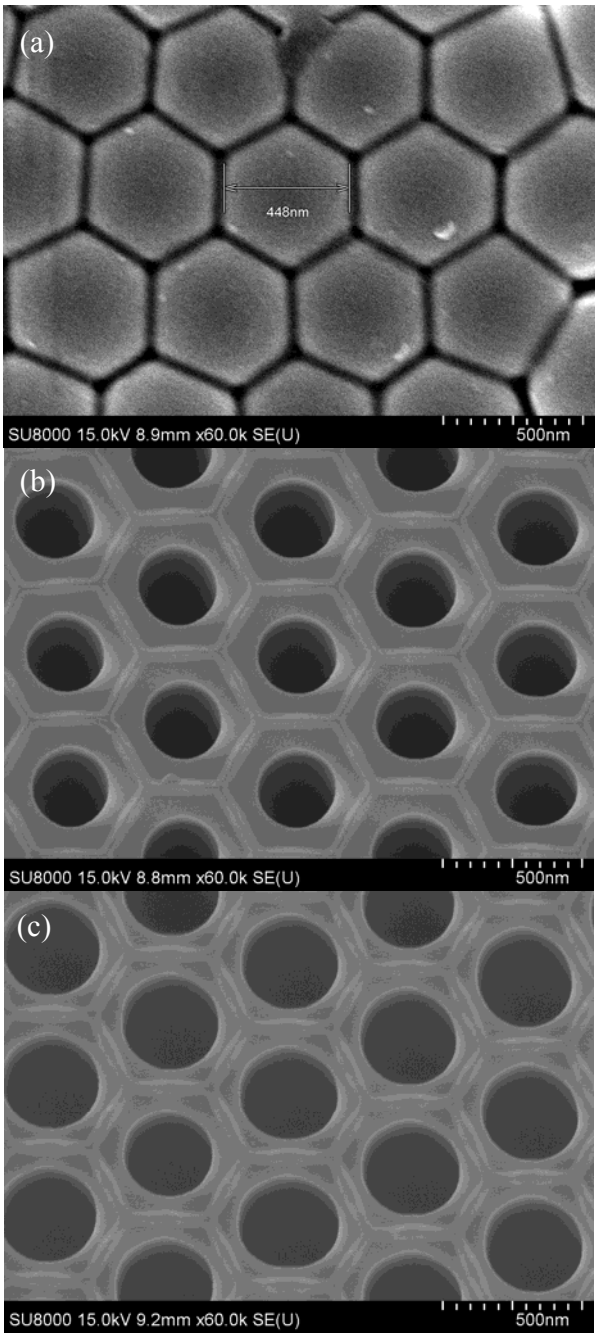

Fig. 1 Bottom images of AAO; (a) barrier layer, (b) honeycomb pores, enlarged pores

It is proposed that the mechanical stress at the metal/oxide

interface causes repulsive force between the neighboring pores which promotes the formation of an ordered hexagonal pore array. The voltage determines the barrier layer thickness and AAO cell size of the film. As two experience formulas can estimate the pore size and the pore distance of AAO. The pore size with voltage is: C=mV, where C is cell size (nm), V is anodizing voltage (V), and m is a constant (2~2.5). The pore distance with voltage is V=(2R-10)/2, where 2R is spacing distance (5~1000 nm).

The thick outer porous layer has morphology of an array of self-organized hexagonal nanopores under suitable conditions of voltage, temperature, current density and electrolytic composition. The films formed in acid solutions below approximately 100 V are generally believed to be completely amorphous. At higher voltages, crystalline forms of γ-alumina are thought to be generated as local islands within the amorphous film.

Fig. 2 showed the top images of AAO. (a) Disordering pores presented after 200 V anodization and the pore sizes are between 300 ~500 nm. (b) Ordering pores present after pore widening process by H_3PO_4 solution, the pore size is 450 nm. (c) AAO film thickness is 256μm, and (d) AAO has straight tube structure. The melting point of the barrier oxide is near 1000 °C, also the AAO template is stable around 800 °C which is lower than that of bulk alumina (2017 °C for $Al_2O_{3(\gamma)}$).

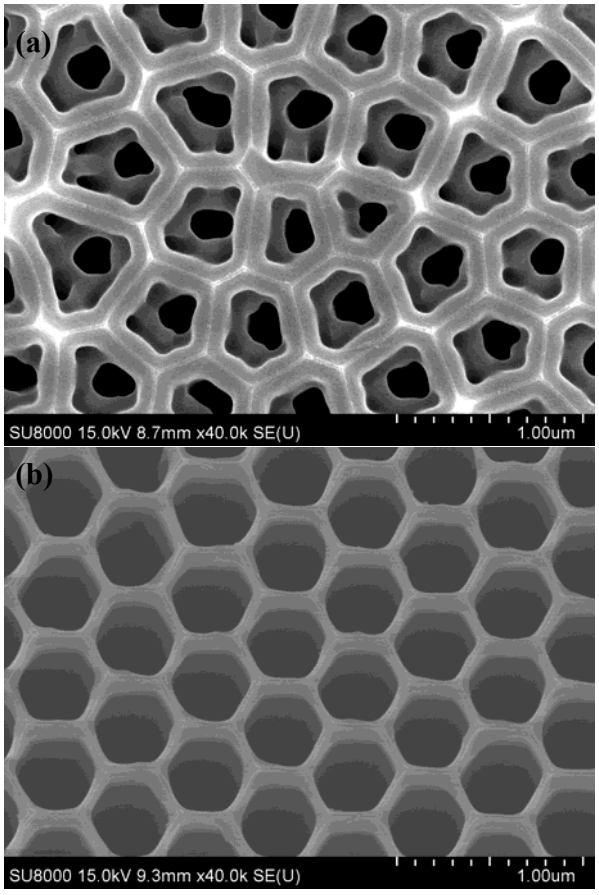

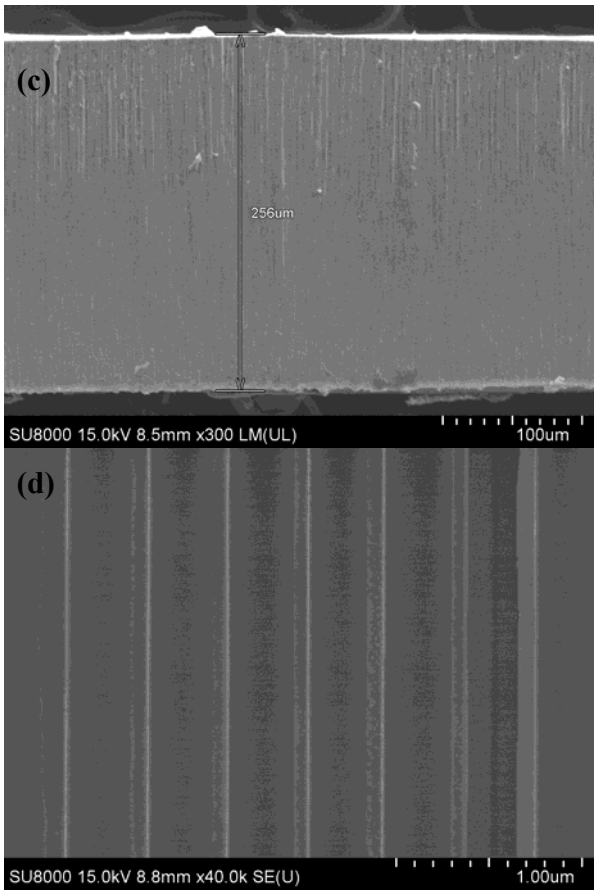

Fig. 2 AAO images; (a) disordering pores, (b) ordering pores, 256 μm film thickness, (d) straight tube structure

Samples of 10 cm ×10 cm size AAO/TiO_2 NT films were loaded into a glass chamber with valves for evacuation and gas feeding. After the samples were loaded, the chamber was evacuated to about 10 mTorr using a mechanical pump and then sealed. The valves were switched to make CO_2 flow first through de-ionized water in a conical flask, and then flow into the reactor. The amount of H_2O vapor in the feed stream (H_2O/CO2 molar ratio) was regulated by the temperature of the water in the conical flask. Carbon dioxide (99.99% pure), via a mass flow controller (MKS instruments), was passed through a bubbler containing de-ionized water before entering the reaction chamber. Both inlet and outlet valves were kept open with the chamber flushed for more than 10 min and then closed, maintaining a nominal excess pressure of less than 1.0 psi. All photocatalytic carbon dioxide conversion experiments were done under AM 1.5 (300 W, 91160-Oriel Solar Simulator, 100 mw cm^{-2}). Reaction products were analyzed using a gas chromatograph equipped with flame ionization (FI) and thermal conductivity (TC) detectors. The FI detector enabled detection of most hydrocarbons, and the TC detector was used for other products. A schematic diagram of the experimental setting is shown in Fig. 3.

Fig. 4 shows (a) top-view and (b) side-view SEM images of Al_2O_3 template made by 1% H_3PO_4 solution and pore widening for 180 min with a tube diameter of 500 nm, and TiO_2 NT

deposited inside Al_2O_3 template. The thickness of the TiO_2 NT pore wall depends on the deposition time. A longer deposition time causes a smaller TiO_2 NT pore size, and a TiO_2 rod presents after a long deposition time. However, the TiO_2 NT surface area is reduced, with increased NT walls [14].

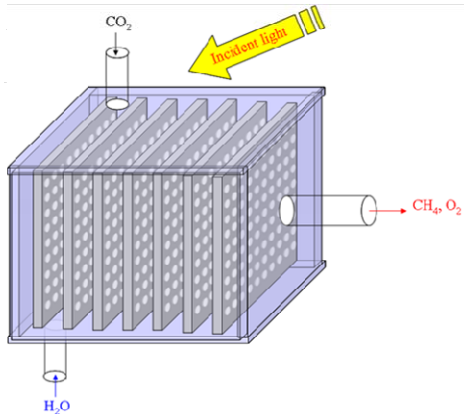

Fig. 3 Schematic diagram of a simple apparatus to measure insulator efficiency and heat transfer coefficient

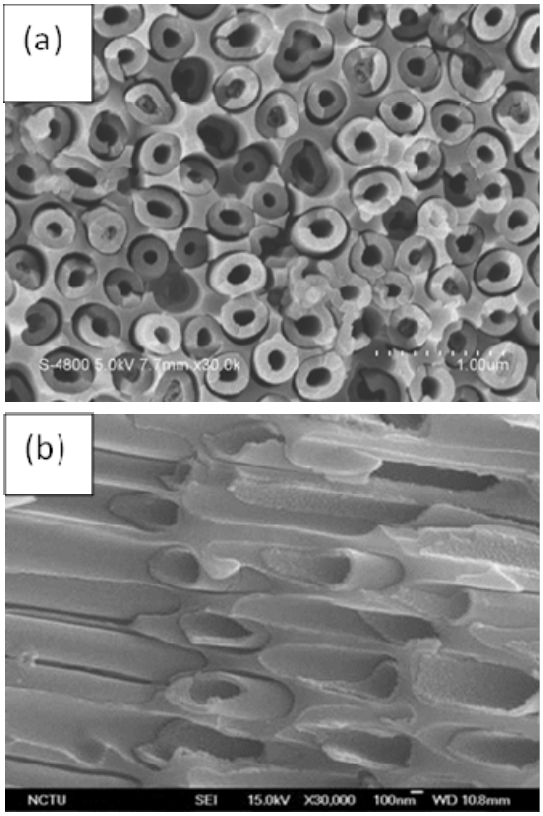

Fig. 4 SEM images of TiO_2 NT in AAO template; (a) top view of TiO_2 NT with 300 nm pore size on AAO template with 500 nm, (b) side view of TiO_2 NTs inside AAO template

IV. Conclusions

Since the Al_2O_3 template process is sensitive to the operation conditions, defects will appear in Al_2O_3 template when unsuitable conditions are used. The conditions include electrolyte temperature, applied voltage, electrolyte composition, electrolyte stirring, and current density distribution. In an anodization process, the working electrode presents an exothermic reaction. Control of electrochemical parameters when preparing small-scale samples for academic research is not difficult. In mass production environments, however, maintenance of constant current density and temperature becomes a critical issue. In this paper we have success made a large size of nano-structure tubular film which is a potential material for green energy application.

Acknowledgment

The authors gratefully appreciate the financial support of the Chung-Shan Institute of Science and Technology (CSIST) under the Contract No. 104-EC-17-A-22-0442.

References

[1] Inoue T, Fujishima A, Konishi S, Honda K, "Photoelectrocatalytic Reduction of Carbon Dioxide in Aqueous Suspensions of Semiconductor Powders", Nature, vol. 277, pp. 637-638, 1979.
[2] Halmann M, Ulman M, Blajeni BA, "Photochemical Solar Collector for The Photoassisted Reduction of Aqueous Carbon Dioxide", Sol. Energy, vol. 31, pp. 429-431, 1983.
[3] Adachi K, Ohta K, Mizuna T, "Photocatalytic Reduction of Carbon Dioxide to Hydrocarbon Using Copper-load Titanium Dioxide", Sol. Energy, vol. 53, pp. 187-190, 1994.
[4] Anpo M, Yamashita H, Ichihashi Y, Ehara S, "Photocatalytic Reduction of CO2 with H2O on Various Titanium Oxide Catalysts", J. Electroanal. Chem., vol. 396, pp. 21-26, 1995.
[5] Thampi KR, Kiwi J, Graetzel M, "Methanation and Photo-methanation of Carbon Dioxide at Room Temperature and Atmospheric Pressure", Nature, vol. 327, pp. 506-508, 1987.
[6] Zumdahl SS, Zumdahl SA, Chemistry, 7TH edition, Houghton Mifflin, New York, USA, pp. 353, 2009.
[7] Ohko Y, Tryk DA, Hashimoto K, Fujishima A, "Autoxidation of Acetaldehyde Initiated by TiO2 Photocatalysis under Weak UV Illumination" , J. Phys. Chem. B, vol. 102, pp. 2699-2704, 1998.
[8] Ishitani O, Inoue C, Suzuki Y, Ibusuki T, "Photocatalytic Reduction of Carbon Dioxide to Methane and Acetic Acid by an Aqueous Suspension of Metal-deposited TiO2", J. Photochem. Photobiol. A: Chem., vol. 72, pp. 269-271, 1993.
[9] Slamet HW, Nasution E, Purnama S, Kosela J, Gunlazuardi J, "Photocatalytic Reduction of CO2 on Copper-doped Titania Catalysts Prepared by Improved-impregnation Method", Catal. Commun.,vol. 6, pp. 313-319, 2005.
[10] Varghese OK, Paulose M, Tempa TJ, Grimes CA, "High-Rate Solar Photocatalytic Conversion of CO2 and Water Vapor to Hydrocarbon Fuels", Nano Letts., vol. 9, pp. 731-737, 2009.
[11] Chen CC, Chen JH, Chao CG, "Post-treatment Method of Producing Ordered Array of Anodic Aluminum Oxide Using General Purity Commercial (99.7%) Aluminum", Jpn. J. Appl. Phys., vol. 44, pp. 1529-1533, 2005.
[12] Chen SH, Chen CC, Luo ZP, Chao CG, "Fabrication and characterization of eutectic bismuth-tin (Bi-Sn) nanowires", Mater. Lett., vol. 63, pp. 1665-1668, 2009.
[13] Chen SH, Chen CC, Chao CG, "Novel Morphology and Solidification Behavior of Eutectic Bismuth-Tin (Bi-Sn) Nanowires", J. Alloys and Compounds, vol. 481, pp. 270-273, 2009.
[14] Chen CC, Cheng CH, Tang G, Lin T, Lin CK, "Template Assisted Fabrication of TiO2 and BaTiO3 Nanotubes", Applied Mechanics and Materials, vol. 271-272, pp. 107-111, 2013.